Available online at www.sciencedirect.com
ScienceDirect
Biosensors and Bioelectronics 22 (2007) 1359–1367
BIOSENSORS & BIOELECTRONICS
www.elsevier.com/locate/bios

Large-conductance cholesterol–amphotericin B channels in reconstituted lipid bilayers

Solomon Yilma [a], Jennifer Cannon-Sykora [b], Alexandre Samoylov [a], Ting Lo [c], Nangou Liu [d], C. Jeffrey Brinker [e], William C. Neely [b], Vitaly Vodyanoy [a,*]

[a] *Department of Anatomy, Physiology and Pharmacology, Auburn University, 109 Greene Hall, Auburn, AL 36849, USA*
[b] *Department of Chemistry, Auburn University, Auburn, AL 36849, USA*
[c] *Department of Electrical Engineering, Auburn University, Auburn, AL 36849, USA*
[d] *University of New Mexico, Center for Micro-Engineered Materials, Albuquerque, NM, USA*
[e] *Sandia National Laboratory, Albuquerque, NM, USA*

Received 5 March 2006; received in revised form 30 May 2006; accepted 7 June 2006
Available online 13 July 2006

Abstract

The antimycotic activity of amphotericin B (AmB) depends on its ability to make complexes sterols to form ion channels that cause membrane leakage. To study this phenomenon, surface pressure (π) as a function of surface area (A) and π–A hysteresis were measured in monolayers of AmB–cholesterol mixtures on the water–air interface. The most stable monolayers were produced from molecules of AmB and cholesterol with 2:1 stoichiometry. At this ratio, AmB and cholesterol interact to form ion channels in lipid bilayers with millisecond dwell times and conductances of 4–400 pS. The AmB–cholesterol complexes assemble in three, four, etc., subunit aggregates to form ion channels of diverse and large-conductances. Their I–V characteristics were linear over a range of ±200 mV. The channel currents were inhibited by the addition of tetraethylammonium (TEA), potassium channel blocker, to the *cis*-side of the membrane. Likewise, AmB–cholesterol complexes reconstituted in membrane-coated nanoporous silicon dioxide surfaces showed single channel behavior with large amplitudes at various voltages. Large-conductance ion channels show great promise for use in biosensors on solid supports.

Keywords: Amphotericin B; Cholesterol; Bilayer; Large ion channel

1. Introduction

Amphotericin B (AmB) is a polyene macrolide antibiotic that is widely used for its antifungal activity, despite its undesirable side effects (Hartsel and Bolard, 1996). In biological systems, AmB acts by forming ion channels that induce ion leakage across lipid membranes (Bolard, 1986; Holz and Finkelstein, 1970). The formation of these channels is highly dependent on the presence of sterols (cholesterol or ergosterol) in the membrane (Kerridge and Whelan, 1983). It has been initially suggested that the channels are composed of AmB–sterol complexes made of superimposed antibiotic and sterol molecules. The polar groups on these molecules face toward the inside of the channel where they interact with water molecules, while the hydrophobic groups interact with the aliphatic chains of membrane phospholipids (DeKruijff and Demel, 1974). Stoichiometries for AmB–sterol complexes ranging from 1:4 to 1:0.7 have been reported (Seoane et al., 1998). The electrophysiological properties of AmB channels in lipid bilayer membranes have been extensively studied in the past in order to elucidate the mechanism of action of AmB. However, the results of these studies, which were performed using various AmB/cholesterol ratios, have primarily revealed channels with conductances less than 70 pS (Ermishkin et al., 1976, 1977; Borisova et al., 1979; Brutyan and McPhie, 1996; Cotero et al., 1998). Our survey of existing literature on AmB channels has failed to reveal any previous observations of larger-conductance AmB channels.

We have previously shown that AmB and cholesterol form a complex with a stoichiometry of 2:1 that can produce highly conductive ion channels in phospholipid bilayers (Sykora et al., 2003). We present further evidence of these channels and their kinetic properties in tip–dip lipid bilayers, as well as pro-

* Corresponding author. Tel.: +1 334 844 5405; fax: +1 334 844 5388.
E-mail address: vodyavi@vetmed.auburn.edu (V. Vodyanoy).

0956-5663/$ – see front matter © 2006 Elsevier B.V. All rights reserved.
doi:10.1016/j.bios.2006.06.004

vide observation of these channels functioning in phospholipid membrane-coated nanoporous silicon dioxide surfaces (Lu et al., 2001; Doshi et al., 2000).

2. Materials and methods

2.1. Materials

Amphotericin B was purchased from Sigma Co. (St. Louis, MO) in powder form. Cholesterol and 1,2-diphytanoyl-*sn*-glycero-3-phosphocholine solutions were purchased from Avanti Polar Lipids (Alabaster, AL). Both were used without further purification. Chloroform (>99% purity), methanol (>99% purity), 2-propanol (99.5% purity), and hexane (>95% purity) were all purchased from Aldrich Chemical Company (Milwaukee, WI) in bottles packaged under nitrogen. TEA was also purchased from Aldrich Chemical Company in crystalline form. Thin nanoporous (∼7 nm pore diameter) silicon dioxide plates were supplied by Dr. C.J. Brinker at the Sandia National Laboratory.

2.2. Studies of amphotericin B/cholesterol mixed monolayers

A series of mixed cholesterol and AmB films, ranging from 0 to 1 mole fraction of AmB were prepared with 2:1 (v/v) chloroform/methanol solvent or 3:1 (v/v) mixture of 2-propanol and water solvent. Cholesterol was dissolved in hexane. The AmB solution was centrifuged at 15,000 × *g* at 4 °C for 1 h to remove any material that did not dissolve. The amount of the AmB in the solution was determined by evaporating a 5 mL sample of the solutions and weighing the residue. The AmB concentration was additionally controlled by monitoring the absorption at 408 nm ($1.3 \times 10^5\ M^{-1}\ cm^{-1}$ extinction coefficient) for the 2-propanol and water solvent (Wojtowicz et al., 1998). A concentration of 0.14 ± 0.011 mg/mL AmB was the highest achieved for the 2-propanol and water solvent. All spreading solvents were stored in the dark in a −20 °C freezer.

The stability of the spreading solutions was controlled by measurements of the electronic absorption spectra measured by a Shimadzu UV-3101PC spectrophotometer over the range of 300–450 nm. The monomeric species of AmB were determined at 365, 385 and 408 nm, while the aggregate form of AmB was resolved at a maximum absorption peak of 340 nm (Romanini et al., 1999).

Free energy of mixing (ΔG_m) was obtained from the surface area–pressure isotherms for monolayers of AmB, cholesterol, and its mixtures as described in (Sykora et al., 2003).

2.3. Reconstitution of amphotericin B–cholesterol channels in lipid bilayers

Lipid bilayers containing pure 1,2-diphytanoyl-*sn*-glycero-3-phosphocholine were formed on the tip of patch pipettes using the tip–dip technique previously described (Suppiramaniam et al., 2001; Vodyanoy et al., 1993). The bilayers were formed in asymmetric saline condition by the successive transfer of two lipid monolayers on the tip of the patch pipette. The external solution (bathing the *cis*-side of the membrane) contained (in mM) 125 NaCl, 5 KCl, 1.25 NaH_2PO_4, and 5 Tris–HCl at pH 7.4, and the internal solution (inside the patch pipette) contained 110 KCl, 4 NaCl, 2 NaH_2CO_3, 0.1 $CaCl_2$, 1 $MgCl_2$, and 2 MOPS at pH 7.4. A 2:1 (mol/mol) mixture of 0.6 μg AmB and 0.12 μg cholesterol dissolved in a chloroform–methanol (2:1, v/v) solvent was sonicated together with 10 μg phospholipid (in hexane) and 10 μL of extracellular solution in order to form liposomes. The emulsion was then carefully transferred to the surface (air–water interface) of the extracellular solution bathing the *cis*-side of the membrane and allowed to equilibrate for 1 min. Incorporation of AmB–cholesterol into the membrane was achieved by dipping the tip of the patch pipette into the emulsion. The membrane incorporated AmB–cholesterol molecules were subjected to conventional electrophysiological (Suppiramaniam et al., 2001; Vodyanoy et al., 1993) studies at room temperature (∼22 °C). The resulting single channel current fluctuations were filtered at 1 or 5 kHz using a lowpass Bessel filter and recorded on VHS tapes for later analysis. Single channel fluctuations elicited by the AmB–cholesterol complexes were subsequently blocked by the addition of TEA to the extracellular solution on the *cis*-side of the membrane.

2.4. Reconstitution of amphotericin B–cholesterol channels on membrane-coated nanoporous surfaces

A 150 μL aliquot of AmB, cholesterol, and 1,2-diphytanoyl-*sn*-glycero-3-phosphocholine mixture (2:1:2, mol/mol ratio, respectively) dissolved in a chloroform/methanol (2:1, v/v) solvent at 0.24 mg/mL concentration was spread on the subphase surface. The solutions were spread on a subphase solution of 55 mM KCl, 0.1 mM $CaCl_2$, 1 mM $MgCl_2$, 4 mM NaCl, and 2 mM 3-(*N*-morpholino)propanesulfonic acid (MOPS) made with deionized doubly distilled water Milli-Q water purification system, Millipore Corp., Bedford, MA) and adjusted to pH 7.4 using KOH. The monolayer was allowed to equilibrate and stabilize for 10 min at 19 ± 0.1 °C. It was then compressed at a rate of 30 mm/min, and a vertical film deposition was carried out at a rate of 4.5 mm/min and a constant surface pressure of 23 mN/m (Fig. 1A). Mixed lipid monolayers were transferred onto (22 mm × 22 mm) thin nanoporous (∼7 nm) silicon dioxide plates (Sandia National Lab). The nanopores were first filled with LB buffer solution before being coated with lipid membranes. The membrane-coated nanoporous plate (substrate) was then secured in place by a plastic cell assembly which isolated the center of the plate with a rubber O-ring (Fig. 1B). The surface of the nanoporous plate was covered with a small pool of 0.1 M KCl buffer solution, and the entire plastic cell assembly was placed inside a grounded metal box that was positioned on an isolation table GS-34 (Newport Corp.). The plastic cell assembly was then connected to an Axopatch 200B patch clamp amplifier (Axon Instruments) by immersing a silver/silver chloride electrode into the small pool (300 μL) of aqueous KCl solution. Current measurements were performed with the voltage clamped at −200 to +200 mV range. The voltage clamp ampli-

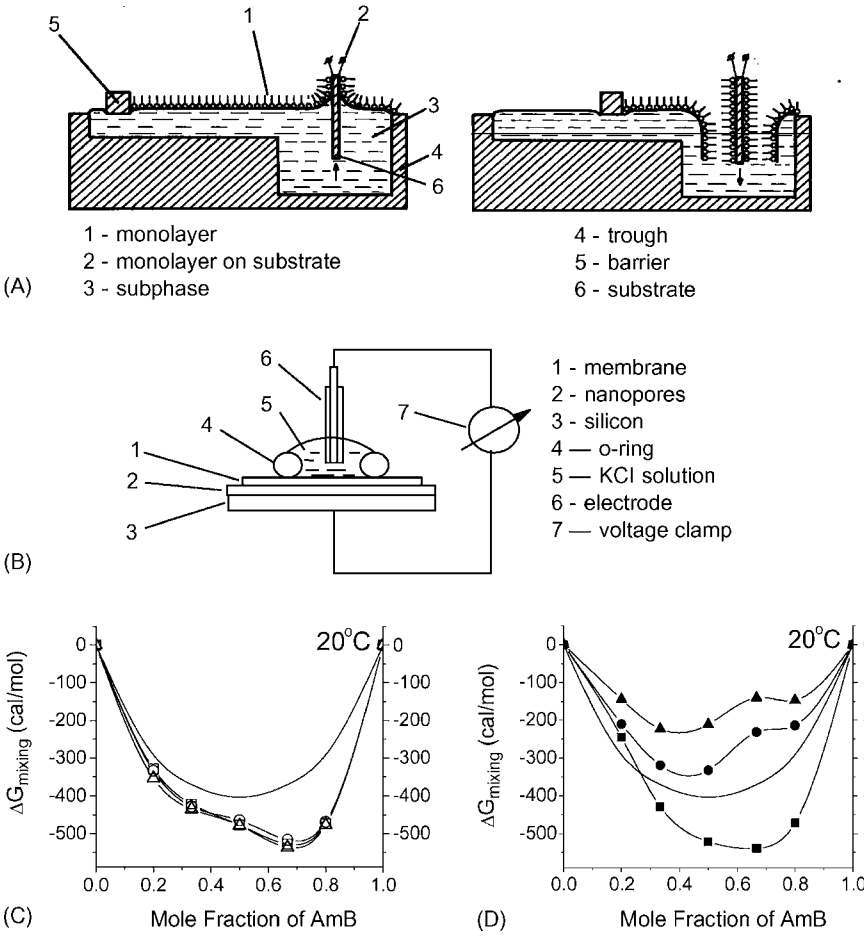

Fig. 1. Monolayer technology. (A) Diagramm of the lipid monolayer/silicon dioxide plate assembly process. (B) Assembly for measurement of currents through ion channels on solid support. (C and D) Free energy of mixing (ΔG_m) as a function of mole fraction AmB. Panel C depicts data from experiments using (2:1) 2-propanol/water spreading solvent at 20 °C. Panel D depicts data from experiments using (3:1) chloroform/methanol spreading solvent at 20 °C. The solid line is for that of an ideal mixture. Symbols represent the following compressions: 0–10 mN/m (squares), 0–20 mN/m (circles), 0–30 mN/m (triangles).

fier was interfaced to a computer with a Digidata 1200 data acquisition board (Axon Instruments).

2.5. Data analysis

Single channel data segments of 5–120 s lengths were digitized at 0.1 ms intervals and transferred to a computer as data files. The data were later subjected to statistical analysis using the Fetchan/Clampfit modules of pCLAMP data analysis program (*Axon Instruments*) as well as the *Microcal* Origin data analysis and technical graphics program.

3. Results

We previously reported that the most stable monolayers were produced when AmB and cholesterol were mixed at 2:1 ratio (Sykora et al., 2003). Fig. 1C and D depict the free energy of mixing (ΔG_M) calculated from pressure–area isotherms and plotted against the mole fraction of AmB along with the free energy of mixing for the ideal system (ΔG_M^I). Free energy values were dependent on composition, spreading solvent, and temperature (Sykora et al., 2003). Significant negative departure of ΔG_M from ideality for monolayers spread from the chloroform/methanol solutions were observed only at low surface pressures (Fig. 1D, lower curves). At higher surface pressures, significant positive departures were observed for the same monolayers (Fig. 1D, upper curves). Different results were obtained using the propanol–water solvent (Fig. 1C). For all surface pressures, the free energy of mixing revealed a minimum at $N_A = 0.667$ (AmB to cholesterol ratio of 2:1). At 20 °C, the negative departure from ideality held for the monolayers of all compositions. As the surface pressure was increased, the free energy values became increasingly negative at all compositions.

When AmB and cholesterol mixed at 2:1 ratio were incorporated into artificial phospholipid bilayer membranes that were formed on the tip of patch pipettes and subjected to electrophysiological studies, ion channel current fluctuations (Fig. 2A–C) with distinct open and closed states were observed. Fig. 2C depicts an expanded segment of the ion channel current data traces in panels A and B to better reveal the distinct states (closed, open level 1, and open level 2) and current fluctuation levels corresponding to large-conductance and smaller-conductance ion channels that were observed in the original data trace at +165 mV. Amplitude distribution analysis (Fig. 2D)

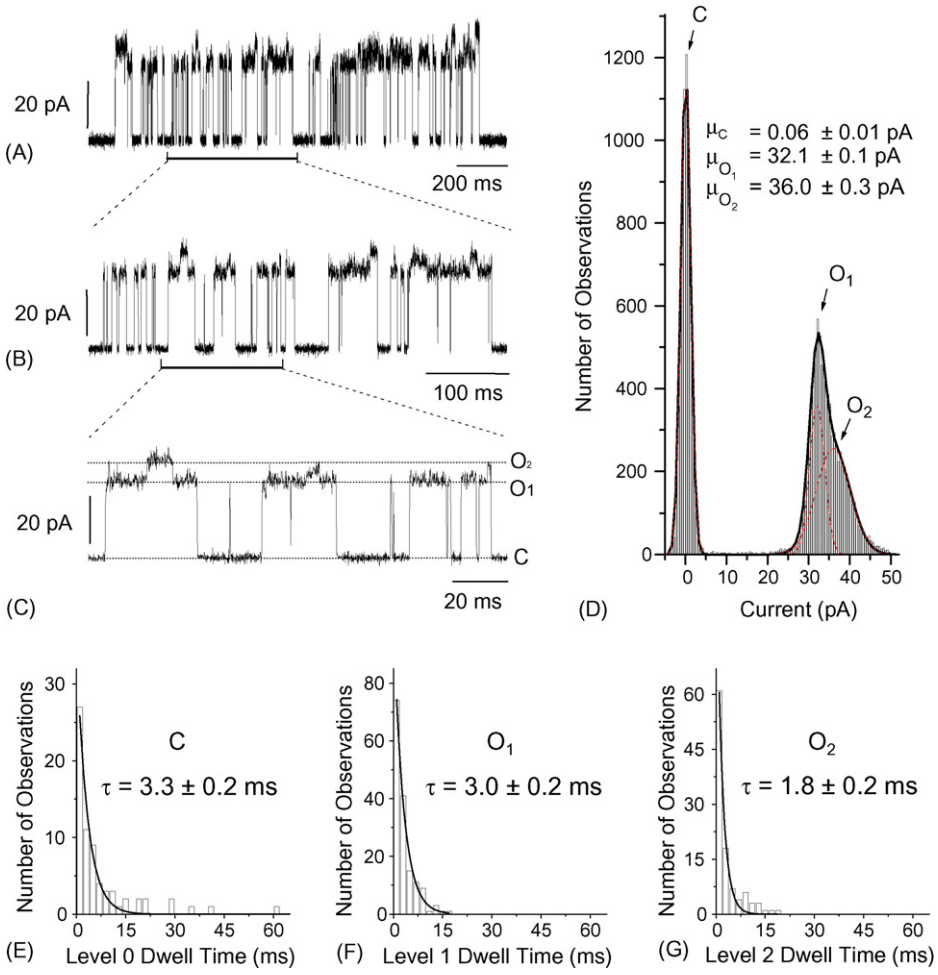

Fig. 2. AmB–cholesterol channels in reconstituted lipid bilayer membranes. (A–C) Ion channel current fluctuations; $V = 165$ mV. Openings are upward. The data traces were sampled at 0.1 ms intervals, filtered at 5 kHz, and plotted as a function of time. (D) Amplitude distribution of channel currents in panel A. (E–G) Dwell time histograms for three different dwell levels.

of the ion channel current trace in Fig. 2A indicates that each state we observed had distinct subpopulations of current levels. Statistical means derived from Gaussian fits ($r^2 = 0.997$) of the subpopulations show that the larger-conductance ion channels had a net current of 32.0 ± 0.1 pA and a calculated relative conductance of approximately 194 pS, while the smaller-conductance ion channels had a net current of 3.9 ± 0.3 pA and a calculated relative conductance of approximately 24 pS (3 experiments). Dwell time analysis (Fig. 2E–G) of each state/current level in the data trace of Fig. 2A produced dwell times of 3.3 ± 0.2 ms ($r^2 = 0.961$), 3.0 ± 0.2 ms ($r^2 = 0.990$), and 1.8 ± 0.2 ms ($r^2 = 0.982$) corresponding to the closed level, open level 1, and open level 2, respectively.

Fig. 3 shows several representative traces of AmB–cholesterol channels with relative conductances between 13 and 191 pS at various voltages. The amplitude distribution histograms (displayed on the right) corresponding to each trace reflect the distinct channel current subpopulations that were observed within each trace. Overall, most of our observations were dominated by larger-conductance channels (greater than 60 pS) that were present either at a single conductance level or superimposed with smaller-conductance channels. Panel A of Fig. 3 depicts a data trace composed of current fluctuations from large-conductance (191 pS) and smaller-conductance (47 pS) channels that opened concurrently and superimposed on each other at +165 mV (4 experiments). Similarly, panel D shows a small-conductance channel (28 pS) superimposed on top of a larger-conductance channel at −52 mV (2 experiments). Conversely, Panel F displays the consistent fluctuation of a small-conductance (13 pS) channel at −168 mV (3 experiments). The rest of the panels (B, C, and E) display the medium to large-conductance channels that were commonly observed in our channel data recordings.

Fig. 3G shows the resulting current–voltage relationship for one group of low conductance AmB–cholesterol channels that were chosen from clearly discernible current fluctuations of channels with relative conductances between 25 and 35 pS. Linear regression fit of the plot ($r^2 = 0.999$) revealed a slope and corresponding average conductance of 28.4 ± 0.6 pS and a reversal potential of 11.2 ± 3.1 mV. Due to the method we employed in pre-grouping the channel currents based on their relative conductance values, we were unable to determine whether

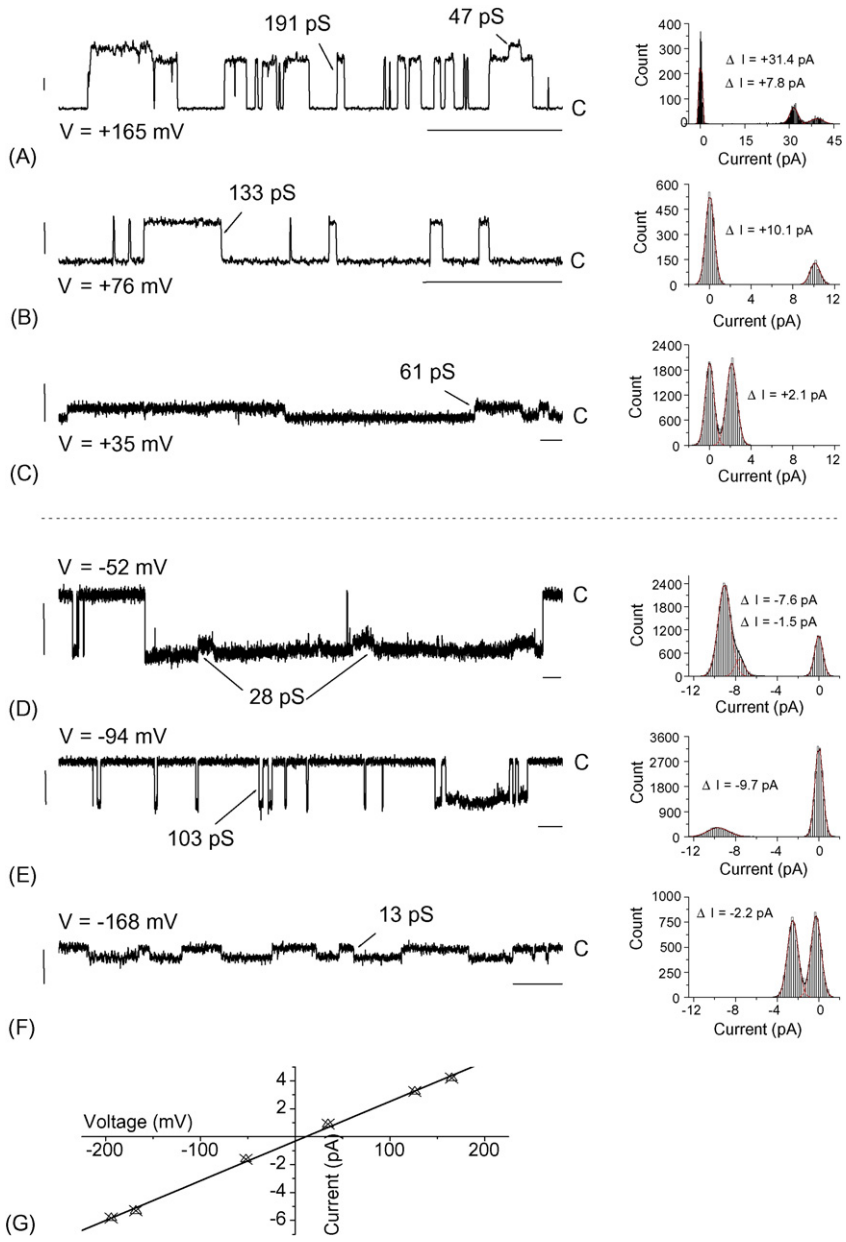

Fig. 3. Diverse conductances of AmB–cholesterol channels. Vertical scale bars = 8 pA; horizontal scale bars = 100 ms. (A–F) current traces at indicated voltages and corresponding amplitude distribution histograms on the right. Panel G shows current–voltage relationships of low conductance AmB–cholesterol channels. The data points were fitted using linear regression ($r^2 = 0.999$, slope = 28.4 ± 0.6 (S.E.) pS, V_{rev} = 11.2 ± 3.1 (S.E.) mV, S.D. = 0.2, $P < 0.0001$).

any of the AmB–cholesterol channels exhibited any rectification that would be reflected by the non-linear appearance of a current–voltage plot.

The diverse conductance of the AmB–cholesterol channels we observed can be effectively explained by a simple model based on a formula that correlates channel conductance with increasing pore size that results as more subunits assemble/polymerize to form larger channels. One subunit is composed of 2 amphotericin B (A) and 1 cholesterol (C) molecules: $2A + C = A_2C$; two subunits are combined give $A_2C + A_2C = A_4C_2$, and so on (Fig. 4A). Using a geometric formula for calculating the area (S) one can estimate the size of the pore inside of the cholesterol–amphotericin B channel:

$$S = \frac{d^2[n\cot(\pi/n) - \pi(n/2 - 1)]}{4} \quad (1)$$

where d is a diameter of one subunit and n is a number of subunits.

The relative channel conductance and the conductance distribution depend on the number of A_2C subunits in one channel. Fig. 4B shows the comparison of the experimental channel conductance and the conductance predicted by this simple space filling model. The experimental values of relative conductance were estimated from experimental amplitude distribution his-

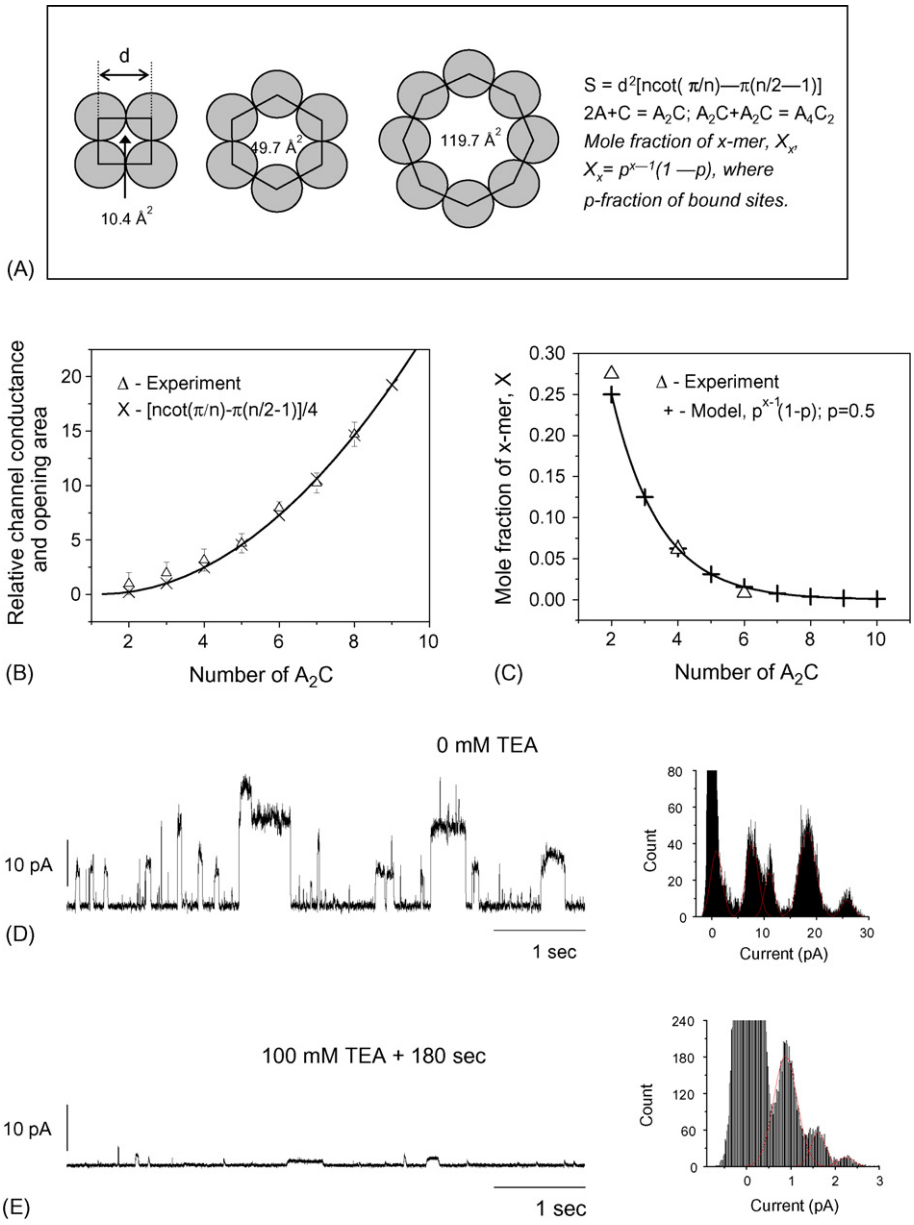

Fig. 4. Properties of AmB–cholesterol channels. (A) Space filling model of AmB–cholesterol channel. (B) Comparison of the channel experimental relative channel conductance and the relative open area predicted by the space filling model as the function of number of subunits (Eq. (1)). Experimental values of conductance were scaled to values of calculated open area (S/d^2, Eq. (1)) C. Relative amplitude distribution of AmB–cholesterol channels and mole fraction of x-mer channels (X_x) as function of number of subunits. $X_x = p^{x-1}(1-p)$, a mol fraction of x-mer channels (Eq. (2)), p is a fraction of bound sites ($p = 0.5$). (D) AmB–cholesterol channel currents in the absence of TEA. The corresponding amplitude distribution histogram (*right panel*) was fitted with the sum of six Gaussian functions ($r^2 = 0.995$) with population means of -0.04 ± 0.00 (S.E.), 0.64 ± 0.06, 7.71 ± 0.04, 11.01 ± 0.05, 18.30 ± 0.03, and 25.90 ± 0.12 pA, respectively. (E) AmB–cholesterol channel currents in the presence of 100 mM TEA. The corresponding amplitude distribution histogram (*right panel*) was fitted with the sum of four Gaussian functions ($r^2 = 0.999$) with population means of 0.03 ± 0.00 (S.E.), 0.88 ± 0.01, 1.62 ± 0.02, and 2.24 ± 0.08 pA, respectively.

tograms for channels composed of consecutive numbers of A_2C subunits.

The function of distribution or the mole fraction x-mer channel (the channel composed of x subunits) can be calculated using the model derived for polymerization of monomer molecules (Tanford, 1961):

$$X_x = p^{x-1}(1-p) \tag{2}$$

where X_x is a mol fraction of x-mer channels, p is a fraction of bound sites. Fig. 4C shows the comparison of the relative amplitude distribution and that predicted by the distribution of x-mer channels for consecutive numbers of A_2C subunits. The experimental values of relative amplitudes were taken from experimental histograms of records containing three discernible peaks.

AmB–cholesterol channels were noticeably inhibited by the application of the potassium ion channel blocker TEA. Fig. 4D and E depict these channels in the absence (D) and presence (E) of 100 mM TEA applied to the extracellular or *cis*-side of the membrane. The amplitude distribution histograms to the

Table 1
Effects of tetraethylammonium on AmB/cholesterol channels

	0 mM TEA	No. of events observed	100 mM TEA	No. of events observed
Channel current population means observed[a]	−0.0 ± 0.0 pA			
	0.6 ± 0.1 pA		−0.0 ± 0.0 pA	
	7.7 ± 0.0 pA		0.9 ± 0.0 pA	
	11.0 ± 0.1 pA		1.6 ± 0.0 pA	
	18.3 ± 0.0 pA		2.2 ± 0.1 pA	
	25.9 ± 0.1 pA			
Maximum channel current population mean[a]	25.9 ± 0.1 pA		2.2 ± 0.1 pA	
Closed level dwell time[b]	66.6 ± 59.5 ms	54	311.1 ± 234.4 ms	16
Open level dwell time[b]	37.6 ± 98.4 ms	54	44.9 ± 97.9 ms	16
Probability for open level[b]	0.36		0.13	

[a] Data obtained from Gaussian function fitting results of amplitude distribution histograms in Fig. 4D and E.
[b] Data obtained from dwell time distribution analysis of traces in Fig. 4D and E.

right of each trace more clearly reflect the channel current levels that were observed in each trace. In the absence of TEA, multiple large-amplitude current levels are apparent. However, in the presence of 100 mM TEA, the multiple large-amplitude current levels are replaced by very small amplitude current fluctuations (Table 1). In addition to inhibiting the current amplitude of AmB–cholesterol channels, TEA also reduced the probability of opening of these channels by altering the average dwell times for both the closed state and open states (Table 1).

We tested the functionality of AmB–cholesterol channels in membranes formed on nanoporous solid surfaces. Electrophysiological studies of 2:1 AmB–cholesterol mixtures that were incorporated into artificial phospholipid membranes formed on the surface of nanoporous (7 nm pore diameter) silicone dioxide plates revealed large amplitude ion channel current fluctuations (Fig. 5A–C) with distinct open and closed states. Fig. 5A shows a data trace (top right panel) containing current fluctuations of AmB–cholesterol channels on membrane-coated nanoporous silicon dioxide surfaces at +200 mV filtered at 1 kHz. Remarkably, the channels exhibited large relative conductance and high noise level for the baseline. Fig. 5B shows the same trace after the noise was partially filtered out using conventional lowpass Bessel filter set to 0.1 kHz. Amplitude distribution analysis of the ion channel current trace in Fig. 5B indicates that each state we observed had distinct subpopulations of current levels that were statistically significant. Statistical means derived from Gaussian fits ($r^2 = 0.992$) of the subpopulations show that these large-conductance ion channels had a net current of 59.9 ± 0.6 pA and a calculated relative conductance of approximately 300 pS. Fig. 5C depicts an expanded segment of the ion channel current data trace in panel B to better reveal the distinct states (closed level and open level) that were observed in the original data trace.

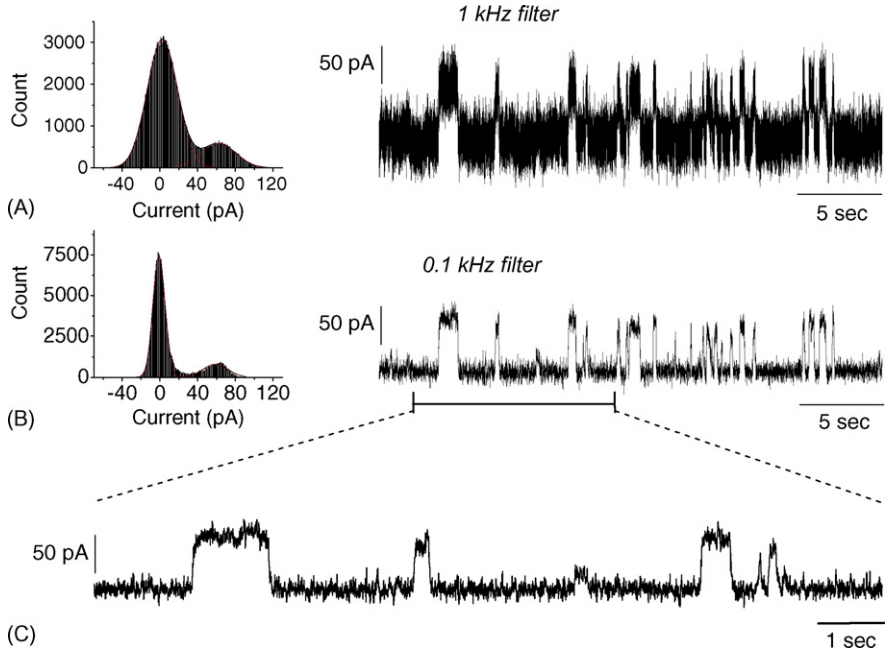

Fig. 5. AmB–cholesterol channels in membrane-coated nanoporous silicon dioxide surfaces. (A) A current trace filtered at 1 kHz and a corresponding amplitude distribution histogram (*top left panel*) was fitted with the sum of two Gaussian functions ($r^2 = 0.999$) with population means of 2.46 ± 0.03 (S.E.) pA and 62.14 ± 0.19 pA, respectively. (B) The same current trace as in A but filtered at 0.1 kHz. (C) An expanded segment of the 0.1 kHz filtered segment in panel B.

4. Discussion

We have previously shown (Sykora et al., 2003) that at low surface pressures at 20 °C the most stable state of the monolayer is achieved at AmB mole fraction of 0.667, which is similar to results of Rey-Gomez-Serranillos et al., 2001). This finding suggests that the most favorable interactions between AmB and cholesterol occur at this mole fraction, thus indicating the formation of a 2:1 AmB–cholesterol complex (Sykora et al., 2003; Brutyan and McPhie, 1996). In our experiments we utilized a 2:1 AmB–cholesterol ratio because the free energy of mixing is minimal (Fig. 1) and the stability of the system is maximized.

AmB ion channels observed in this work were of unusually large-conductance, reaching up to 400 pS. These channels were composed of AmB and cholesterol molecules assembled with 2:1 stoichiometry. The conductances observed in our experiments were very high compared to AmB channel conductances previously observed in 0.5-mm and 0.25 diameter black lipid membranes made from *n*-hexane (Ermishkin et al., 1976) and *n*-heptane (Borisova et al., 1979) solutions of brain extraction (2–8 pS), in 0.1–0.3 mm diameter solvent-free synthetic phospholipid-cholesterol membranes (4–23 pS) (Brutyan and McPhie, 1996), and in tip–dip patch pipette bilayers made of a synthetic phospholipid with and without cholesterol (2–70 pS) (Cotero et al., 1998). We did observe lower conductance channels, however, the larger channel conductance levels were dominant and more prevalent in our experiments. We attribute the large channel conductance to the precise 2:1 ratio of the AmB and cholesterol mixture used in our experiments and to the prefabrication in liposomes of AmB/cholesterol channels prior to their reconstitution in bilayers (Sykora et al., 2003; Vodyanoy et al., 1993).

The varying conductance of AmB–cholesterol channels observed in our experiments suggest that individual AmB–cholesterol complexes (we will refer to them as subunits) assemble in three, four, five, etc., subunit aggregates to form ion channels of varying pore sizes and conductance in lipid bilayers. As more subunits assemble to form channels with larger pore diameters, the channel conductance increases accordingly. A similar idea by Bolard et al. (1990) suggests that the various conductance levels observed for AmB channels in lipid membranes can be attributed to the formation of channels of different sizes and may have their origin in the procedure employed in introducing the AmB into the membranes. It is likely that our technique promoted the formation of channels with various pore sizes by allowing the AmB–cholesterol complex to aggregate and preassemble while still in the small area of the lipid bilayer membrane of the liposomes. A microscopic electrostatic model of AmB channels proposed by Bonilla-Marin et al. (1991) also reinforces the idea that the AmB channels of different pore sizes are formed by a variable number of subunits.

The significant diversity in the conductance of AmB–cholesterol channels observed in our experiments can be effectively explained by a mathematical model that correlates the number of subunits in a channel and the resulting pore size with the relative conductance of the channel.

AmB–cholesterol channels observed in our experiments were significantly inhibited by the potassium ion channel blocker TEA. This finding was consistent with observations of various groups (Ermishkin et al., 1977; Cohen, 1986; Gadzhi-Zade, 1983; Brutyan, 1982) that applied TEA to AmB–cholesterol channels. The effect we observed was gradual and peaked at 3 min after applications of the compound to the *cis*-side of the membrane. The before-and-after effect of our observation actually created the appearance that high conductance channels were inhibited or somehow modified to appear like low conductance channels after the application of TEA. Similar phenomenon were observed by Borisova et al. (1979) who showed that TEA blocking efficiency varies with the initial conductance of the channel, and went on to propose that the blocking efficiency of compounds on the conductance of AmB channels increased as the size of the blocking molecule approached the pore diameter of the AmB channel. TEA is about the same size as a hydrated K^+ ion ($r \sim 4.13$ Å) and carries the same +1 electric charge (Hille, 1984). The apparent sizes of 3-mer and 4-mer AmB channel are ~4 and 6.2 Å, respectively. Gadzhi-Zade (1983) speculated that the TEA molecule does not move through the channel, but instead sits at the mouth of the channel and blocks ion flow through the pore. TEA also reduced the probability of opening of the AmB–cholesterol channels by altering the average dwell times for both the closed state and open states.

Efforts to construct ion-channel-based stochastic sensors (Bayley et al., 2000; Schuster et al., 1998; Gu et al., 1999) in recent years have shed light on the potential for ion channels for use as powerful transducers in biosensors. However, this effort has just began addressing the need to devise a stable substrate for supporting these ion channels, as well as constructing a microarray that is practical (Bayley and Cremer, 2001).

Our observations of the functioning of AmB–cholesterol channels on membrane-coated nanoporous silicon surfaces (Lu et al., 2001) indicate that such substrates provide a practical medium for supporting ion channels and ion-channel-based stochastic sensors (Bayley and Cremer, 2001). Similar to the results we obtained in tip–dip membranes, voltage-clamp studies of AmB–cholesterol channels in membrane-coated nanoporous silicon surfaces revealed large channels with ~400 pS relative conductance. The baseline noise observed from these membrane-coated nanoporous silicon surfaces was considerably higher. Understandably, this phenomenon was due to the increased total membrane surface area, capacitance of pores, and the seal resistance (Rudy and Iverson, 1992) in the nanoporous surfaces compared to the significantly smaller surface area of singular tip–dip membranes. Still, with additional filtering, the baseline membrane noise can be reduced to better reveal the channel current fluctuations.

It is worth mentioning that the large-conductance AmB–cholesterol channels were dominant in the membrane-coated nanoporous silicon surfaces. This could be attributed to two factors. The small surface area of the membranes in the individual nanopore structures could serve to promote/support larger-conductance channels by physically crowding smaller channels in favor of larger channels (up to a certain size) which have a smaller circumference to pore-size ratio. Conversely, the current

fluctuations of smaller channels that were present in the medium could have been concealed by the high baseline membrane noise, and subsequently eliminated as artifacts during additional filtering.

Our findings emphasize the importance of employing high conductance ion channels to overcome a low signal to noise ratio in ion-channel-based biosensor. Membrane-coated nanoporous silicon surfaces show great promise for use as mediums for ion-channel-based biosensors as well as for organization in microarrays.

Acknowledgments

We thank Randy O. Boddie for technical assistance. This work was supported by grants from DARPA MDA972-00-1-0011, FAA 01-G-022, US Army N66001-1099-0072, Aetos Technologies, Inc., and by the Auburn University Peaks of Excellence Program in conjunction with the Auburn University Detection and Food Safety Center.

References

Bayley, H., Braha, O., Gu, L.Q., 2000. Stochastic sensing with protein pores. Adv. Mater. 12, 139–142.

Bayley, H., Cremer, P.S., 2001. Stochastic sensors inspired by biology. Nature 413, 226–230.

Bolard, J., 1986. How do the polyene macrolide antibiotics affect the cellular membrane properties? Biochim. Biophys. Acta 864, 257–304.

Bolard, J., Legrand, P., Heitz, F., Cybulska, B., 1990. One-sided action of amphotericin B on cholesterol-containing membranes is determined by its self-association in the medium. Biochemistry 30, 5707–5715.

Bonilla-Marin, M., Moreno-Bello, M., Ortega-Blake, I., 1991. A microscopic electrostatic model for the amphotericin B channel. Biochim. Biophys. Acta 1061, 65–77.

Borisova, M.P., Ermishkin, L.N., Silberstein, A.Y., 1979. Mechanism of blockage of amphotericin B channels in a lipid bilayer. Biochim. Biophys. Acta 553, 450–459.

Brutyan, R.A., McPhie, P.J., 1996. On the one-sided action of amphotericin B on lipid bilayer membranes. J. Gen. Physiol. 107, 69–78.

Brutyan, R.A., 1982. Amphotericin B-induced channels in a lipid bilayer in response to unilateral application. Biofizika 27, 646–649.

Cohen, B.E., 1986. Concentration- and time-dependence of amphotericin-B induced permeability changes across ergosterol-containing liposomes. Biochim. Biophys. Acta 857, 117–122.

Cotero, B.V., Rebolledo-Antunez, S., Ortega-Blake, I., 1998. On the role of sterol in the formation of amphotericin B channel. Biochim. Biophys. Acta 1375, 43–51.

DeKruijff, B., Demel, R.A., 1974. Polyene antibiotic–sterol interactions in membranes of Acholesplasma laidlawii cells and lecithin liposomes. III. Molecular structure of the polyene antibiotic–cholesterol complexes. Biochim. Biophys. Acta 339, 57.

Doshi, D.A., Huesing, I.K., Lu, M., Fan, H., Lu, Y., Simmons-Potter, K., Potter, B.G., Hurd, A.J., Brinker, J., 2000. Optically defined multifunctional patterning of photosensitive thin-film silica mesophases. Science 290, 107–111.

Ermishkin, L.N., Kasumov, K.M., Potseluyev, V.M., 1977. Properties of amphotericin B channels in a lipid bilayer. Biochim. Biophys. Acta 470, 357–367.

Ermishkin, L.N., Kasumov, Kh.M., Potseluyev, V.M., 1976. Single ionic channels induced in lipid bilayers by polyene antibiotics amphotericin B and nystatine. Nature 262, 698–699.

Gadzhi-Zade, Kh.A., 1983. Electric potential at the entrance of the amphotericin channel. Biofizika 28, 999–1001.

Gu, L.Q., Braha, O., Conlan, S., Cheley, S., Bayley, H., 1999. Stochastic sensing of organic analytes by a pore-forming protein containing a molecular adapter. Nature 398, 686–690.

Hartsel, S.C., Bolard, J., 1996. Amphotericin B: new life for an old drug. Trends Pharmacol. Sci. 17, 445–449.

Hille, B., 1984. Ionic Channels of Excitable Membranes, first ed. Sinauer, Sunderland, MA.

Holz, R., Finkelstein, A., 1970. The water and nonelectrolyte permeability induced in thin membranes by the polyene antibiotics nystatin and amphotericin B. J. Gen. Physiol. 56, 125–145.

Kerridge, D., Whelan, W.L., 1983. In: Trinici, A.P.J., Ryley, J.F. (Eds.), Mode of Action of Anti-fungal Agents. Cambridge University Press, Cambridge, pp. 343–375.

Lu, Y., Yang, Y., Sellinger, A., Lu, M., Huang, J., Fan, H., Haddad, R., Lopez, G., Burns, A.R., Sasaki, D.Y., Shelnutt, J., Brinker, C.J., 2001. Self-assembly of mesoscopically ordered chromatic polydiacetylene/silica nanocomposites. Nature 410, 913–917.

Rey-Gomez-Serranillos, I., Dynarowicz-Latka, P., Minones, J., Seoane, R., 2001. Desorption of amphotericin B from mixed monolayers with cholesterol at the air/water interface. J. Colloid Interface Sci. 234, 351–355.

Romanini, D., Avalle, G., Nerli, B., Pico, G., 1999. Thermodynamic and spectroscopic features of the behavior of amphotericin B in aqueous medium. Biophys. Chem. 77, 69–77.

Rudy, B., Iverson, L.E., 1992. Ion Channels, Methods in Enzymology, vol. 207. Academic Press, pp. 45–48.

Schuster, B., Pum, D., Braha, O., Bayley, H., Sleytr, U.B., 1998. Self-assembled a-hemolysin pores in an S-layer-supported lipid bilayer. Biochim. Biophys. Acta 1370, 280–288.

Seoane, R., Minones, J., Conde, O., Casas, M., Iribarnegaray, E., 1998. Molecular organization of amphotericin B at the air-water interface in the presence of sterols: a monolayer study. Biochim. Biophys. Acta 1375, 73–83.

Suppiramaniam, V., Bahr, B.A., Sinnarajah, S., Owens, K., Rogers, G., Yilma, S., Vodyanoy, V., 2001. Member of the ampakine class of memory enhancers prolongs the single channel open time of reconstituted AMPA receptors. Synapse 40, 154–158.

Sykora, J., Yilma, S., Neely, W.C., Vodyanoy, V., 2003. Amphotericin B and cholesterol in monolayers and bilayers. Langmuir 19, 858–864.

Tanford, C., 1961. Physical Chemistry of Macromolecules. Wiley, New York.

Vodyanoy, V., Bahr, B.A., Suppiramaniam, V., Hall, R.A., Baudry, M., Lynch, G., 1993. Single channel recordings of reconstituted AMPA receptors reveal low and high conductance states. Neurosci. Lett. 150, 80–84.

Wojtowicz, K., Gruszecki, W.I., Walicka, M., Barwicz, J., 1998. Effect of amphotericin B on dipalmitoylphosphatidylcholine membranes: calorimetry, ultrasound absorption and monolayer technique studies. Biochim. Biophys. Acta 1373, 220–226.